The Glycosylphosphatidyl Inositol-anchored Adhesion Molecule F3/Contactin Is Required for Surface Transport of Paranodin/Contactin-associated Protein (caspr)

Catherine Faivre-Sarrailh,* France Gauthier,* Natalia Denisenko-Nehrbass,‡ André Le Bivic,* Geneviève Rougon,* and Jean-Antoine Girault‡

*Laboratoire de Génétique et Physiologie du Développement, UMR 6545 CNRS, IBDM, 13288 Marseille, France; and ‡Institut National de la Santé et de la Recherche Médicale (INSERM) U563 and INSERM U114, Collège de France, 75231 Paris, France

Abstract. Paranodin/contactin-associated protein (caspr) is a transmembrane glycoprotein of the neurexin superfamily that is highly enriched in the paranodal regions of myelinated axons. We have investigated the role of its association with F3/contactin, a glycosylphosphatidyl inositol (GPI)-anchored neuronal adhesion molecule of the Ig superfamily. Paranodin was not expressed at the cell surface when transfected alone in CHO or neuroblastoma cells. Cotransfection with F3 resulted in plasma membrane delivery of paranodin, as analyzed by confocal microscopy and cell surface biotinylation. The region that mediates association with paranodin was mapped to the Ig domains of F3 by coimmunoprecipitation experiments. The association of paranodin with F3 allowed its recruitment to Triton X-100–insoluble microdomains. The GPI anchor of F3 was necessary, but not sufficient for surface expression of paranodin. F3-Ig, a form of F3 deleted of the fibronectin type III (FNIII) repeats, although GPI-linked and expressed at the cell surface, was not recovered in the microdomain fraction and was unable to promote cell surface targeting of paranodin. Thus, a cooperative effect between the GPI anchor, the FNIII repeats, and the Ig regions of F3 is required for recruitment of paranodin into lipid rafts and its sorting to the plasma membrane.

Key words: neurexin • GPI anchor • lipid rafts • myelination • node of Ranvier

Introduction

During myelination, specialized membrane domains are generated by the contact between axon and glial cells. Cell adhesion molecules (CAMs)[1] and channels are enriched at distinct sites in the node of Ranvier and the paranodes. The voltage-gated sodium channels are concentrated in the nodal region (Waxman and Ritchie, 1993), together with isoforms of two proteins of the Ig superfamily, NrCAM and neurofascin (Davis et al., 1996). The lateral diffusion of these transmembrane proteins may be limited by their association with ankyrin-G, a spectrin-binding protein (Zhang and Bennett, 1998). The sequence of events observed during myelination indicates that clustering of NrCAM and neurofascin precedes clustering of sodium channels and ankyrin G (Lambert et al., 1997). The nodes of Ranvier are flanked by paranodal regions where the terminal loops of myelinating glial cells are in close interaction with the axolemma. Voltage-gated potassium channels are concentrated in the juxtaparanodal region (Wang et al., 1993), whereas paranodin, a transmembrane neuronal glycoprotein of the neurexin superfamily, is highly enriched in the paranodal regions (Menegoz et al., 1997). Paranodin was also cloned independently as a protein associated with F3/contactin and termed caspr (contactin-associated protein; Peles et al., 1997). During development, paranodin/caspr is first uniformly expressed on the surface of axons and dendrites and later, as myelination occurs, its distribution becomes restricted to the paranodal region of the axons (Einheber et al., 1997; Menegoz et al., 1997). Paranodin contains an NH_2-terminal discoidin domain, two epidermal growth factor (EGF)-like regions flanked by laminin-G domains, characteristic of the neurexin superfamily, followed by a transmembrane domain and a short cytoplasmic tail (Fig. 1). The cytoplasmic tail con-

Address correspondence to Catherine Faivre-Sarrailh, Laboratoire de Génétique et de Physiologie du Développement, UMR 6545 CNRS, IBDM, Parc Scientifique de Luminy, 13288 Marseille cedex 9, France. Tel.: 33-4-9126-9736. Fax: 33-4-9126-9748. E-mail: sarrailh@lgpd.univ-mrs.fr

[1]*Abbreviations used in this paper:* CAM, cell adhesion molecule; caspr, contactin-associated protein; EGF, epidermal growth factor; FNIII, fibronectin type III; GNP, glycophorin C, neurexin IV, paranodin motif; GPI, glycosylphosphatidyl inositol; PI-PLC, phosphatidyl inositol-phospholipase C; TX-100, Triton X-100.

tains a juxtamembrane sequence encompassing a GNP (glycophorin C, neurexin IV, paranodin) motif able to bind band 4.1 domains (Girault et al., 1998). These domains are named after a protein first identified in erythrocytes in which it participates in the anchoring of cortical actin cytoskeleton to the membrane (for recent reviews see Girault et al., 1998, 1999). Band 4.1 domain is also found in ezrin, radixin, and moesin (ERM proteins), as well as in many other proteins, including FAK and JAK, defining a domain superfamily referred to as band 4.1/JEF (JAK, ERM, FAK; Girault et al., 1998, 1999). These domains appear to be often involved in reversible interactions with membrane proteins. Paranodin does indeed bind to proteins of the band 4.1 family (Menegoz et al., 1997; Denisenko-Nehrbass, N., T. Galvez, and J.-A. Girault, unpublished observations) and this interaction provides a potential link with the cytoskeleton, which might result in the formation of a barrier to lateral diffusion of axolemmal proteins. Paranodin is closely related to *Drosophila melanogaster* neurexin IV, a component of fly septate junctions, which has been demonstrated to be essential for dorsal closure of the embryo and axonal insulation in the peripheral nervous system (review in Bellen et al., 1998). Recent work has revealed that paranodin/caspr is a member of a family of proteins including axotactin (Yuan and Ganetzky, 1999) and caspr 2 (Poliak et al., 1999).

Paranodin/caspr interacts with contactin/F3/F11, a glycosylphosphatidyl inositol (GPI)-anchored glycoprotein of the Ig superfamily, when the two proteins are expressed in the same cells (cis-interaction; Peles et al., 1997). F3 displays a modular structure composed of six Ig domains and fibronectin type III (FNIII) repeats (Fig. 1) known to interact with multiple ligands (reviews in Brümmendorf and Rathjen, 1996; Faivre-Sarrailh and Rougon, 1997). It must be pointed out that F3 is able to bind, in addition to paranodin, to other axonal glycoproteins specifically expressed at the node of Ranvier, including NrCAM and neurofascin (Volkmer et al., 1996, 1998). F3 also mediates trans-interactions between neuron and glia, since it binds tenascin-C and RPTPβ/ζ (Peles et al., 1995; Revest et al., 1999) expressed at the surface of astrocytes. Finally, F3 interacts with tenascin-R, an extracellular matrix component secreted by oligodendrocytes, which may act as a functional modulator of sodium channels (Xiao et al., 1999). Thus, F3 appears to have a much wider spectrum of distribution and interactions than paranodin. On the other hand, paranodin provides F3 with a potential link with intracellular structural or signaling molecules. In the present study, we analyzed the functional role of the association between F3 and paranodin, focusing on the targeting of the two proteins. Using double-transfected CHO and neuroblastoma cells lines, we demonstrated that the GPI-anchored glycoprotein F3 is critically involved in the surface transport of paranodin via the glycosphingolipid-cholesterol rafts.

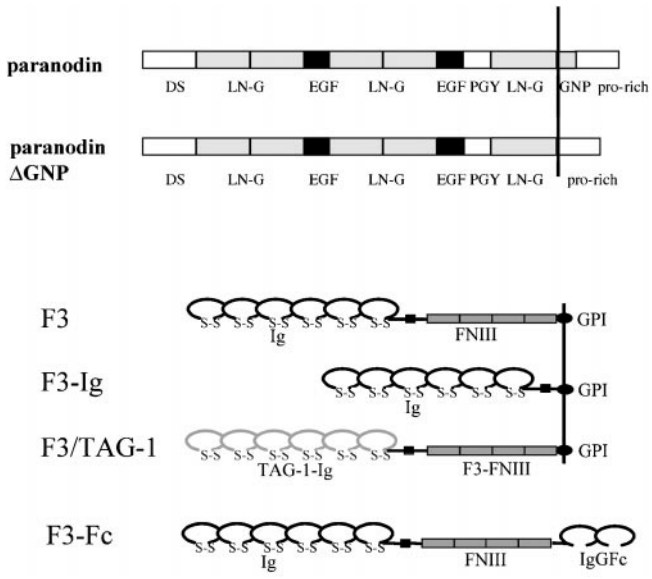

Figure 1. Schematic structure of paranodin, F3, and of their mutated or chimeric forms. The main domains of paranodin are indicated: DS, discoidin domain; EGF, EGF-like sequences; LN-G, laminin-G domain; PGY, Pro-Gly-Tyr repeats; pro-rich, proline-rich region. ParanodinΔGNP is deleted from the band 4.1 binding region (i.e., GNP motif conserved between glycophorin C, neurexin IV and paranodin). The F3 molecule contains six Ig domains and four FNIII repeats. The F3-Ig construct is deleted from the four FNIII repeats. The F3/TAG-1 construct corresponds to the six Ig domains of TAG-1 fused with the four FNIII repeats and the GPI anchor of F3. F3Fc is a chimera between the Ig and FNIII domains of F3 and the Fc fragment of human IgG.

Materials and Methods

Antibodies

For immunofluorescence microscopy and immunoblotting, we used a rabbit antiserum prepared against the F3 Ig-like domains designated 24 (Gennarini et al., 1991). Rabbit antiserum SL23, which was raised against a 6× His-tag fusion protein encompassing residues 841–1,380 of paranodin, reacted with epitopes in its extracellular region. Rabbit antiserum SL51, which was raised against a GST-fusion protein encompassing residues 1,303–1,380 of paranodin, reacted with epitopes in its intracellular region (Menegoz et al., 1997). Immunoprecipitation and immunoblotting were performed with SL51, immunofluorescence was carried out on permeabilized cells with SL51 or on living cells with SL23. Monoclonal anti-RER antibody was purchased from Dako. Monoclonal antigiantin was a gift from Dr. H.P. Hauri (Biozentrum, Basel, Switzerland). Monoclonal anti-LAMP1 antibody (AC17) was used as a lysosome marker (Nabi et al., 1991). Rabbit anti–TAG-1 antiserum (TG3) was a gift from D. Karagogeos (University of Crete Medical School, Heraklion, Greece). Peroxidase-, FITC-, and Texas red-conjugated immunoglobulins were purchased from Jackson ImmunoResearch.

Expression Constructs

The DNA constructs pRc-CMV/F3, pRc-CMV/F3Ig (Durbec et al., 1994), pIG/F3 (Revest et al., 1999), and pC-TAG (Buttiglione et al., 1998) were described previously. The construct pMV/TAG-F3, which contains the Ig domains of the rat TAG-1 sequence 1–1,904 fused with the FNIII region and the GPI anchor of the rat F3 sequence 1775 to 3611 cloned in the eucaryotic expression vector pMV7 was a gift from Dr. A. Furley (University of Sheffield, Sheffield, UK). The construct pBK-CMV/Pnd consisted of the entire coding region of the rat paranodin (Menegoz et al., 1997) cloned into pBK-CMV2, a vector modified from pBK-CMV (Stratagene) by deletion of an Nhe1-Sal1 fragment corresponding to the bacterial promoter. The construct pBK-CMV/PndΔGNP was deleted of the bases coding for amino acid residues 1,306–1,328, which encompass the GNP motif responsible for the binding of band 4.1 domains (Girault et al., 1998).

Recombinant Cell Lines

CHO, COS-7, and N2a neuroblastoma cells were grown in DME (GIBCO BRL) containing 10% FCS, supplemented with penicillin (50 U/ml) and streptomycin (50 μg/ml). CHO cell lines stably expressing F3, F3-Ig (Dur-

bec et al., 1992, 1994), or TAG-1 (Buttiglione et al., 1998) were described previously. Stable paranodin-expressing CHO lines were obtained by transfection of 2×10^5 cells with 4 μg pBK-CMV/Pnd using lipofectamine (GIBCO BRL) and selection with G418. Stable CHO cell lines coexpressing paranodin and F3 were obtained by transfection of the 1A F3-transfected clone with 4 μg of pBK-CMV/Pnd, together with 200 ng pSV2*gpt* using selection with 0.05 mg/ml mycophenolic acid in 0.25 mg/ml xanthine and 15 μg/ml hypoxanthine medium. Isolated clones obtained by limiting dilution were analyzed by immunofluorescence.

Neuroblastoma N2a cells were transiently transfected using Fugene-6 (Roche).

Indirect Immunofluorescence

For the visualization of paranodin transfected in CHO and N2a cells, using the antiserum directed against the intracytoplasmic region, cells were fixed with methanol for 10 min at −20°C, rehydrated in PBS, incubated with SL51, diluted 1:2,000 in PBS containing 3% BSA for 1 h, rinsed with PBS, incubated with Texas red-conjugated anti-rabbit immunoglobulins (diluted 1:100) in PBS containing 3% BSA for 1 h. After washing with PBS, cells were mounted in Mowiol (Calbiochem). Double-immunofluorescence staining for paranodin and RER, giantin, or LAMP-1 was realized after methanol fixation. Immunofluorescence staining for paranodin using antiserum SL23 (diluted 1:200), directed against the extracellular part of the molecule, was carried out on live CHO cells in control conditions or after 16-h treatment with 10^{-4} U/ml phosphatidyl inositol-phospholipase C (PI-PLC; Oxford GlycoSystems). Cells were then fixed with 4% paraformaldehyde in PBS, washed, and incubated with Texas red-conjugated anti-rabbit immunoglobulins (diluted 1:100). To determine the percentage of transiently transfected N2a cells coexpressing F3 or TAG-1 and paranodin, double-staining with anti-F3 (1:200) or anti–TAG-1 antibodies (1:1,000) and paranodin was performed. Live cells were first processed for F3 or TAG-1 immunofluorescence, as described above. Cells were then fixed with 4% paraformaldehyde in PBS and permeabilized with 0.1% Triton X-100 (TX-100) in PBS, and antiparanodin immunostaining was carried out using SL51 antiserum. CHO or N2a cells were examined using a confocal laser scanning microscope (Zeiss). Cells were optically sectioned in the xy plane (parallel to the substratum) using 63× NA 1.4 objective and minimum slice thickness of 0.3 μm, with multiple scan averaging. Recording was performed using excitation wavelength of 543 nm and a 570-nm long pass filter. For CHO cells, simultaneous two-channel recording was performed using excitation wavelengths of 488/543 nm, a 515–525 band pass FITC filter, together with a 570-nm long pass filter.

Immunoblot Analyses of Low Density TX-100 Insoluble Complexes from Transfected CHO Cell Lines

Low density TX-100–insoluble complexes were prepared as previously described (Olive et al., 1995). CHO cells (10^7) in 2 ml of 25 mM MES, pH 6.5, containing 0.15 M NaCl, 1% TX-100, and protease inhibitors (1 mM PMSF, 5 μg/ml α-2-macroglobulin, 1 μg/ml leupeptin, and 5 μg/ml pepstatin). The extract adjusted to 40% sucrose was placed at the bottom of a 5–30% linear sucrose gradient and centrifuged at 4°C for 17 h at 39,000 rpm in a SW41 Beckman rotor. Fractions (1 ml) were collected, analyzed by 7% PAGE, and immunoblotted for F3 and paranodin. After electrotransfer to nitrocellulose membrane (Amersham) and blocking in PBS containing 3% BSA, proteins were detected by incubation with rabbit antiparanodin (1:2,000) or anti-F3 (1:500) immune sera overnight at 4°C and peroxidase-conjugated anti-rabbit immunoglobulins (1:10,000) for 1 h at room temperature. Bound antibodies were revealed using peroxidase substrate kit (Dako) or chemiluminescence (Roche).

Immunoprecipitation

Double-transfected CHO or COS-7 cells were lysed for 30 min on ice with 50 mM Tris, pH 7.5, 1% NP-40, containing 10 mM $MgCl_2$ and protease inhibitors centrifuged at 4°C for 15 min at 15,000 rpm. Aliquots of the supernatant were analyzed by immunoblotting for F3 or TAG-1. After preclearing for 2 h at 4°C with protein A–Sepharose, the supernatant was immunoprecipitated for 2 h at 4°C, with protein A–Sepharose coated with SL51 (5 μl). The beads were washed twice with 50 mM Tris, 150 mM NaCl, and 1% NP-40, and twice with 50 mM Tris and 150 mM NaCl. Immune precipitates were analyzed by immunoblotting with antiparanodin, anti-F3, or anti–TAG-1 antibodies.

Cell Surface Biotinylation

Transfected CHO cells were washed three times for 10 min with PBS at 4°C, and then biotinylated with 0.5 mg/ml sulfo-NHS-LC-biotin (Pierce) in 10 mM triethanolamine, pH 9, 140 mM NaCl for 20 min at 4°C. After two washes in PBS at 4°C, cells were lysed in 50 mM Tris, pH 7.4, 1% BSA, 1% NP-40, and protease inhibitors. Immunoprecipitation of paranodin was carried out as described above and immune precipitates were analyzed by immunoblotting with antiparanodin antibodies or peroxidase-conjugated streptavidine.

Results

Association with F3 Mediates the Cell Surface Sorting of Paranodin in Transfected CHO Cells

Paranodin was stably transfected in CHO cells. Three independent clones were selected, which exhibited >50% of cells expressing paranodin (Fig. 2 A) as determined using immunofluorescence staining with antiparanodin antiserum directed against the intracytoplasmic region of the molecule. The immunostaining for paranodin was not observed at the cell membrane, but appeared to be associated with the ER. Similar results were obtained in transiently transfected COS-7 cells (Galvez, T., and J.-A. Girault, unpublished observations). Moreover, only a very faint immunofluorescence staining was detected on live cells when using antiparanodin antiserum SL23 raised against the ectodomain (Fig. 2, B and C).

To test the possible function of the interaction between paranodin and F3, CHO transfectants expressing both glycoproteins were obtained. The F3-transfected CHO clone 1A (Durbec et al., 1992) was transfected with paranodin, together with a pSV2gpt plasmid for selection with mycophenolic acid. Three clones were selected, which were composed of 95% F3-positive cells among which 40–50% were also paranodin-positive. As shown in Fig. 2 D, the plasma membrane was delineated after immunostaining for paranodin using SL51 against the intracellular domain, in all double-transfected cells of the three lines (Fig. 2 D). Moreover, a strong immunostaining for paranodin was observed at the cell surface in double-transfected cells, using SL23 against the ectodomain (Fig. 2, E and F). The SL51 antiserum has been characterized previously (Menegoz et al., 1997). The specificity of the SL23 antiserum was determined using immunoblotting (Fig. 3 C). A single band of ~180 kD was detected in lysate from paranodin-transfected, but not from control COS-7 cells. Moreover, no immunostaining was detected using either SL23 or SL51 antisera on mock- or F3-transfected CHO cells (not shown).

The absence of paranodin surface expression in single-transfected CHO cells could result from either its intracellular retention during biosynthesis or from its intense internalization. Double-immunofluorescence staining supported the first hypothesis, revealing that paranodin was colocalized with ER marker (Fig. 2, G and H), whereas it had a distribution different from that of markers for the lysosomes (Fig. 2 I) and Golgi complex (Fig. 2 J).

To analyze the steady-state distribution of paranodin, surface biotinylation was performed on single- and double-transfected CHO cell lines. Cells were extracted with NP-40 and paranodin was immunoprecipitated. The total amount of paranodin immunoprecipitated in each cell line was determined by immunoblotting (Fig. 3 A) and the bio-

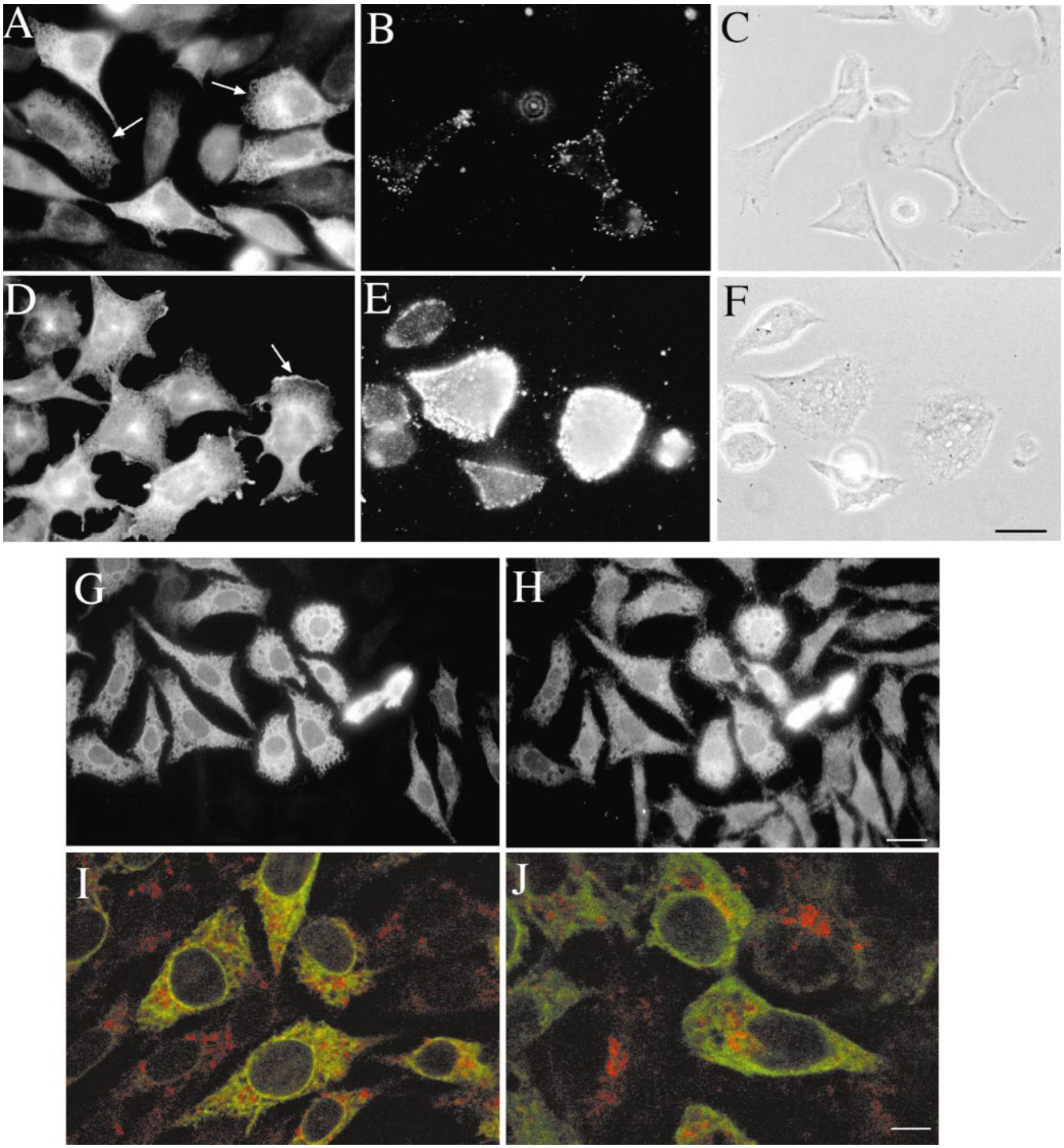

Figure 2. Immunofluorescence analysis of paranodin localization in single- and double-transfected CHO cells. CHO cells stably transfected with paranodin (clone 1-1; A–C) or cotransfected with paranodin and F3 (clone 2-6; D–F) were immunostained for paranodin. A and D, after methanol fixation, cells were immunostained using an antiparanodin antiserum directed against the intracytoplasmic domain. The plasma membrane (arrows in A and D) was delineated by paranodin immunofluorescence in double-transfected cells, but not in single-transfected cells. B and E, Live cells were immunostained using an antiparanodin antiserum directed against the ectodomain. Micrographs were taken using the same exposure time (30 s) in B and E. C and F, corresponding phase contrast. G–J, Analysis of the intracellular distribution of paranodin in single-transfected CHO cells. Double-immunofluorescence indicated that paranodin (G) colocalized with RER marker (H). Confocal analysis of double-immunofluorescence staining for paranodin (in green) and the lysosome marker LAMP1 (in red; I), or Golgi complex marker giantin (in red; J). Paranodin expression was not found in lysosomes or Golgi complex. Paranodin was revealed using FITC-conjugated anti–rabbit immunoglobulins and RER, lysosome, and Golgi complex markers using Texas red-conjugated anti–mouse immunoglobulins. Bars: (A–F) 10 μm; (G and H) 20 μm; (I and J) 3 μm.

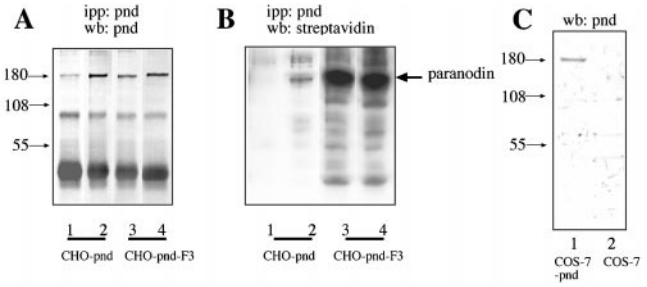

Figure 3. Analysis of steady-state surface expression of paranodin in single- and double-transfected CHO cells. Cells were grown at confluency and biotinylated. After cell lysis, paranodin immune precipitates were analyzed by immunoblotting for paranodin (A) or incubated with peroxidase-conjugated streptavidin revealed by chemiluminescence (B). Lanes 1 and 2, CHO cells stably transfected with paranodin, clones 2-8 (lane 1) and 1-1 (lane 2). Lanes 3 and 4, CHO cells double-transfected with F3 and paranodin, clones 1-8 (lane 3) and 2-6 (lane 4). Paranodin was expressed at the cell surface only in CHO cells cotransfected with F3. C, Immunoblot for paranodin using antiserum L23. 20 μg lysate protein from paranodin-transfected (lane 1) and control (lane 2) COS-7 cells. Molecular mass markers in kD are indicated on the left.

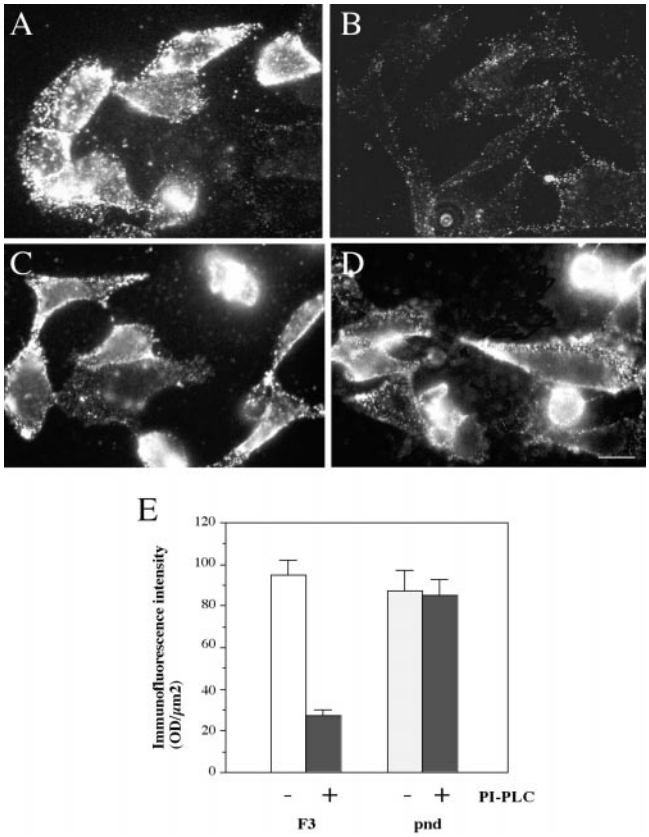

Figure 4. PI-PLC removal of F3 did not modify surface expression of paranodin. Double-transfected CHO cells (clone 2-6) were treated for 18 h without (A and C) or with (B and D) PI-PLC. Live cells were immunostained for F3 (A and B) or paranodin using an antiserum directed against the ectodomain (C and D). Micrographs were taken using the same exposure time (30 s) in A–D. Bar, 10 μm. E, Quantitative analysis of immunofluorescence intensities for F3 and paranodin (pnd), treated without and with PI-PLC. Optical densities (OD/μm^2) were obtained for >20 cells in each experimental condition using NIH image software.

tinylated fraction was revealed using peroxidase-conjugated streptavidin (Fig. 3 B). We found that only a small fraction of paranodin was biotinylated in paranodin-expressing CHO cells. By contrast, a large pool of the molecule was biotinylated in double-transfected CHO cells expressing similar amounts of total paranodin, demonstrating its presence at the cell surface.

To address the question of whether paranodin is stabilized at the cell surface when associated with F3, double-transfected CHO cells were treated with PI-PLC, an enzyme that specifically cleaves GPI anchors. After a 16-h treatment with PI-PLC, expression of GPI-anchored F3 was greatly reduced (73%) at the surface of CHO cells when compared with control conditions (Fig. 4, A, B, and E). In contrast, immunofluorescence for the paranodin ectodomain was unaffected by PI-PLC treatment (Fig. 4, C–E), indicating that the presence of F3 is required for the expression of paranodin at the cell surface, but not for its stabilization at the plasma membrane. Altogether, these data indicate that paranodin expressed alone in CHO cells is retained in the ER and that the presence of F3 prevents this intracellular accumulation and leads to the plasma membrane delivery of paranodin.

Association with F3 Is Necessary for Expression of Paranodin at the Surface of N2a Neuroblastoma Cells

Paranodin is normally expressed in neurons and the lack of membrane localization observed in transfected CHO cells could be due to the fact that these cells are very different from neurons. To rule out this possibility, the cellular distribution of paranodin was analyzed in the N2a neuroblastoma cell line transiently transfected with paranodin alone or in association with F3. Cells permeabilized and immunostained with antibodies directed against the intracytoplasmic domain of paranodin were examined by confocal microscopy (Fig. 5). As in CHO cells, paranodin expressed alone displayed an intracellular localization in all N2a cells examined (>50 cells; Fig. 5 A). When cells were double-transfected, we controlled that all cells expressing paranodin were also positive for F3 using double-immunofluorescence staining (illustrated in Fig. 5, B and C). In cells coexpressing F3, paranodin was almost entirely distributed at the cell membrane (Fig. 5, D and E). Quantitative analysis indicated that 91% of double-transfected N2a cells exhibited immunolocalization for paranodin at the cell membrane (>50 cells examined). As a control for the specificity of the effects of F3, N2a cells were cotransfected with paranodin and TAG-1, a GPI-anchored glycoprotein of the Ig-superfamily that has a high degree of structural homology with F3 (Furley et al., 1990). As shown in Fig. 5, F and G, paranodin distribution was not modified by the coexpression of TAG-1 in all N2a cells observed.

Paranodin contains a conserved GNP sequence in its short intracytoplasmic region that binds band 4.1, a cytoskeleton-anchoring protein (Menegoz et al., 1997; Girault et al., 1998). To investigate whether this motif was in-

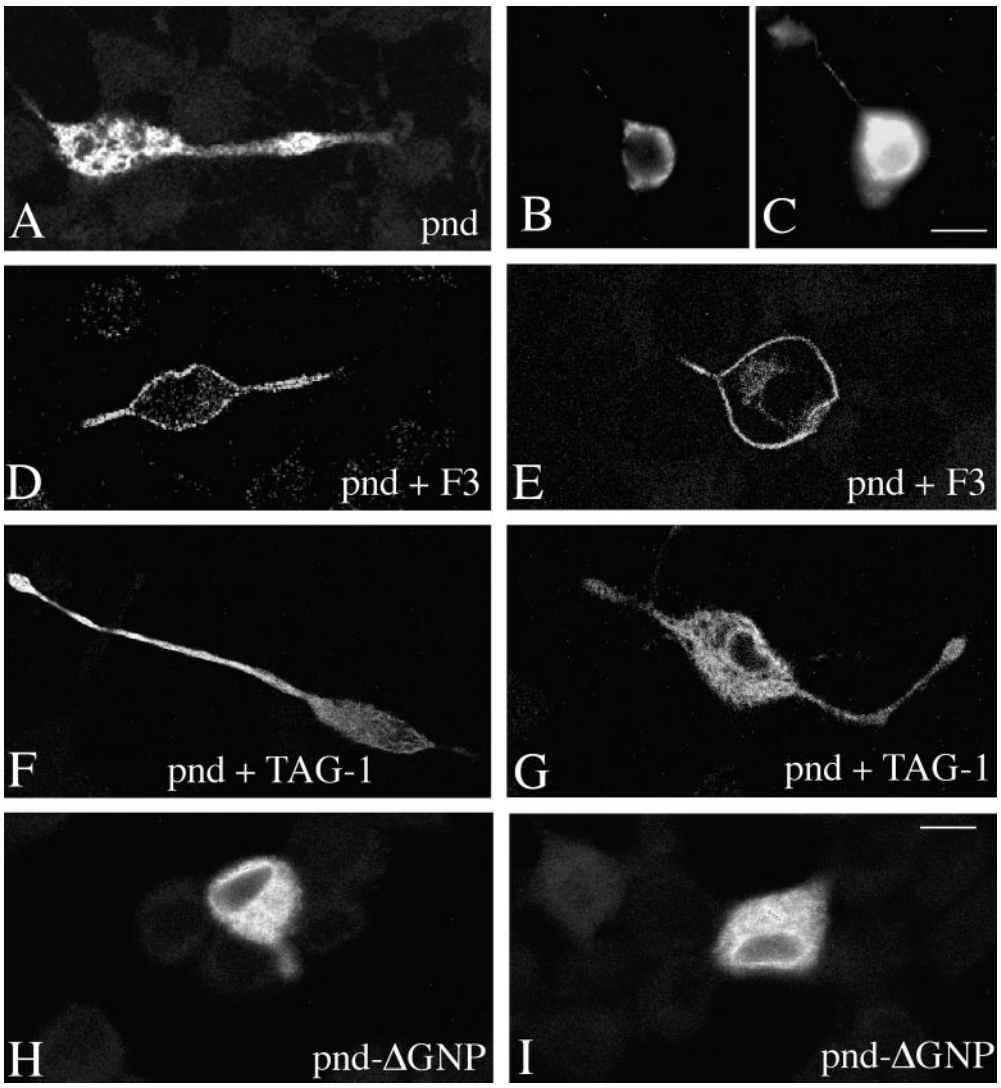

Figure 5. Confocal analysis of paranodin distribution in N2a neuroblastoma cells. N2a were transiently transfected with paranodin (A), paranodin and F3 (B–E), paranodin and TAG-1 (F and G), or paranodin-ΔGNP, which lacks the band 4.1 binding region (H and I). B and C, To control the percentage of cells expressing both F3 and paranodin in double-transfection experiments, live cells were immunostained for F3 (B) and then fixed with 4% paraformaldehyde, permeabilized with 0.1% TX-100, and immunostained for paranodin (C). A and D–I, 48 h after transfection cells were fixed with methanol and immunostained with an antiserum directed against the intracytoplasmic region of paranodin. Cells were optically sectioned in the x-y plane in eight slices (1-μm thick) to visualize paranodin distribution through the entire cell thickness and a representative image was selected. Paranodin (A) and paranodin-ΔGNP (H and I) were only detected in the cytoplasm. Cotransfection with TAG-1 did not modify the intracellular distribution of paranodin (F and G), whereas paranodin was almost entirely detected at the plasma membrane in the presence of F3 (D and E). Experiments were performed in triplicate; >50 cells were analyzed in each experimental condition. Bars: (A and D–I) 10 μm; (B and C) 20 μm.

volved in the intracellular retention of paranodin, the PndΔGNP construct was generated (see Fig. 1). When transfected in N2a cells, PndΔGNP was detected in the cytoplasm, but not at the plasma membrane by confocal analysis (Fig. 5, H and I) in all cells examined, ruling out a role for the association with band 4.1-like proteins in the intracellular retention of paranodin.

F3 Recruits Paranodin into the TX-100–insoluble Microdomains

As a GPI-anchored glycoprotein, F3 has been shown to be enriched in the low density TX-100–insoluble glycosphingolipid microdomains, also called lipid rafts, from neurons and transfected CHO cells (Olive et al., 1995; Buttiglione et al., 1998). During their transport to the surface of epithelial cells, GPI-anchored molecules become insoluble in TX-100 at the level of the Golgi complex (Brown and Rose, 1992). Microdomain association of GPI-anchored molecules mediated by the lipid anchor may be a determinant for delivery to the cell surface and was found to lead to apical sorting in polarized epithelial cells (Lisanti et al., 1989). We tested whether paranodin could be addressed to the cell surface via the lipid rafts when coexpressed with F3. CHO cells stably transfected with paranodin were extracted with TX-100 and subjected to an equilibrium sucrose gradient centrifugation. As expected for a transmembrane molecule, paranodin was entirely recovered in the high density sucrose fractions in the three paranodin-expressing CHO cell lines (Fig. 6 A). In contrast, in double-transfected cell lines, large amounts of paranodin were detected in the low sucrose buoyancy fractions (Fig. 6 B). As previously reported (Olive et al., 1995), F3 was also found in the low buoyancy fractions (Fig. 6 C). These results were reproduced with the three independent double-transfected CHO cell lines. It is thus likely that the recruitment of paranodin into microdomains resulted from its association with F3. To confirm the hypothesis, double-

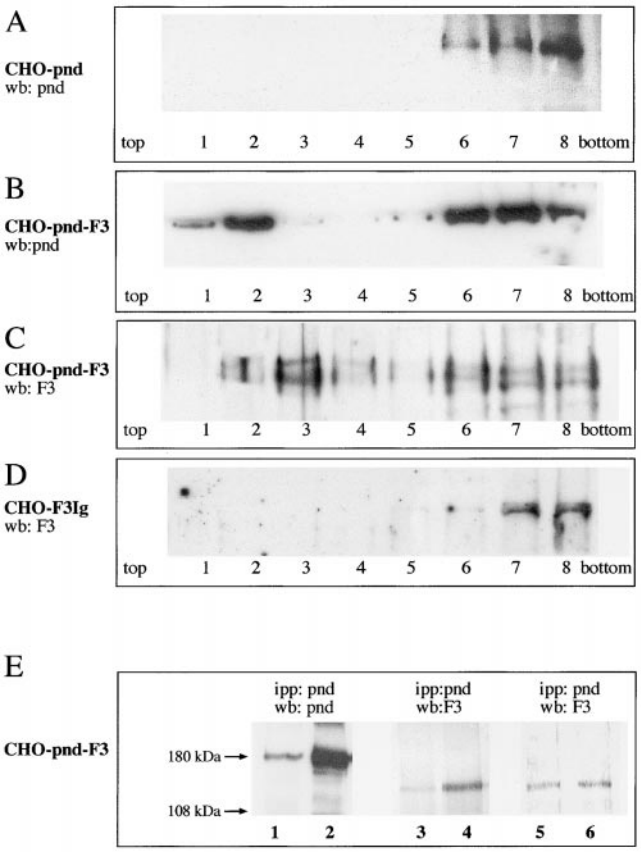

Figure 6. F3 led to the recruitment of paranodin into the glycosphingolipid microdomains in transfected CHO cells. CHO cells transfected with paranodin (clone 1-1; A), paranodin and F3 (clone 2-6; B and C), and F3-Ig (clone B21; D) were lysed with TX-100 and subjected to an equilibrium centrifugation on a gradient of sucrose 5–30%. Fractions of 1 ml were collected and analyzed by SDS-PAGE and immunoblotting for paranodin (A and B) or F3 (C and D). Paranodin was recovered in the first fractions, corresponding to the low density TX-100–insoluble microdomains at the top of the sucrose gradient, in double-transfected CHO cells (B), but not in cells transfected with paranodin only (A). F3 (C), but not F3-Ig (D), was recovered at the top of the sucrose gradient. Note that B and C correspond to different experiments. E, CHO cells double-transfected with paranodin and F3 (clone 1-8, lanes 1 and 3; clone 2-6, lanes 2 and 4) were lysed with NP-40 and immunoprecipitated using antiparanodin antiserum. Immune precipitates were analyzed by immunoblotting for paranodin (lanes 1 and 2) and F3 (lanes 3 and 4). Note that the amount of coprecipitated F3 from the two clones was proportional to the amount of immunoprecipitated paranodin. In some experiments, cells were incubated for 30 min before lysis in the absence (lane 5) or the presence (lane 6) of 10 mM methyl β-cyclodextrin to remove cholesterol from the plasma membrane. Cells were then lysed with NP-40 and immunoprecipitated using antiparanodin antiserum. The amount of F3 in the immune precipitate was analyzed by immunoblotting.

transfected CHO cells were lysed with NP-40, as GPI-anchored glycoproteins can be extracted with this detergent, and immunoprecipitated with antiparanodin antibodies. Immunoblotting analysis of the immune precipitates indicated that F3 associated with paranodin. Moreover, the amount of F3 recovered in the immune precipitates correlated with the amount of paranodin expressed by the different cell lines (Fig. 6 E). To determine whether the association between F3 and paranodin was dependent upon the recruitment of both molecules in sphingolipid-cholesterol rafts, cells were depleted from cholesterol using methyl-β-cyclodextrin. As shown in Fig. 6 E, this treatment did not prevent F3 to be associated with paranodin in the immune precipitates.

The Ig Domains of F3 Are Sufficient for its Interaction with Paranodin

To determine the region in F3 that mediates association with paranodin, COS-7 cells were cotransfected with paranodin and F3, or F3-Ig, a truncated form of F3 lacking the FNIII repeats (see Fig. 1). 48 h after transfection, cells were lysed with NP-40, immunoprecipitated with antiparanodin antibodies, and the immune precipitates were analyzed by immunoblotting. F3 cotransfected with paranodin was recovered in the paranodin immune precipitate (Fig. 7 A). Transfected TAG-1, which is closely related to F3, did not coprecipitate with paranodin (Fig. 7 B). When parano-

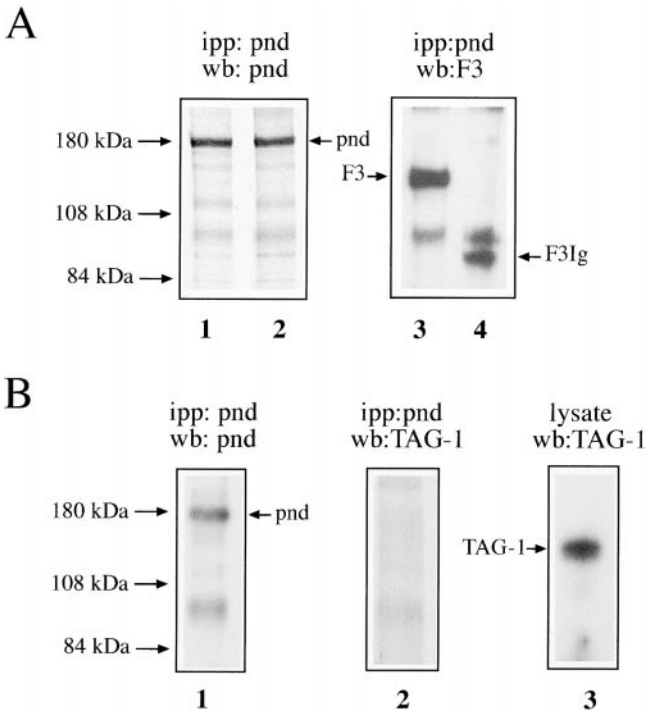

Figure 7. A, Coimmunoprecipitation of F3 and F3-Ig with paranodin in double-transfected COS-7 cells. COS-7 cells were transiently transfected with paranodin and F3 (lanes 1 and 3) or paranodin and F3-Ig (lanes 2 and 4). 48 h after transfection, cells were lysed with NP-40 and immunoprecipitated using antiparanodin antiserum. Immune precipitates were analyzed by immunoblotting for paranodin (lanes 1 and 2) and for F3 (lanes 3 and 4). B, COS-7 cells were transfected with paranodin and TAG-1. Paranodin immune precipitates were analyzed by immunoblotting for paranodin (lane 1) and TAG-1 (lane 2). Expression of TAG-1 was analyzed in 20 μg protein of NP-40 lysates from transfected COS-7 cells by immunoblotting for TAG-1 (lane 3). TAG-1 was not detected in the paranodin immune precipitates. Molecular weight markers are indicated on the left.

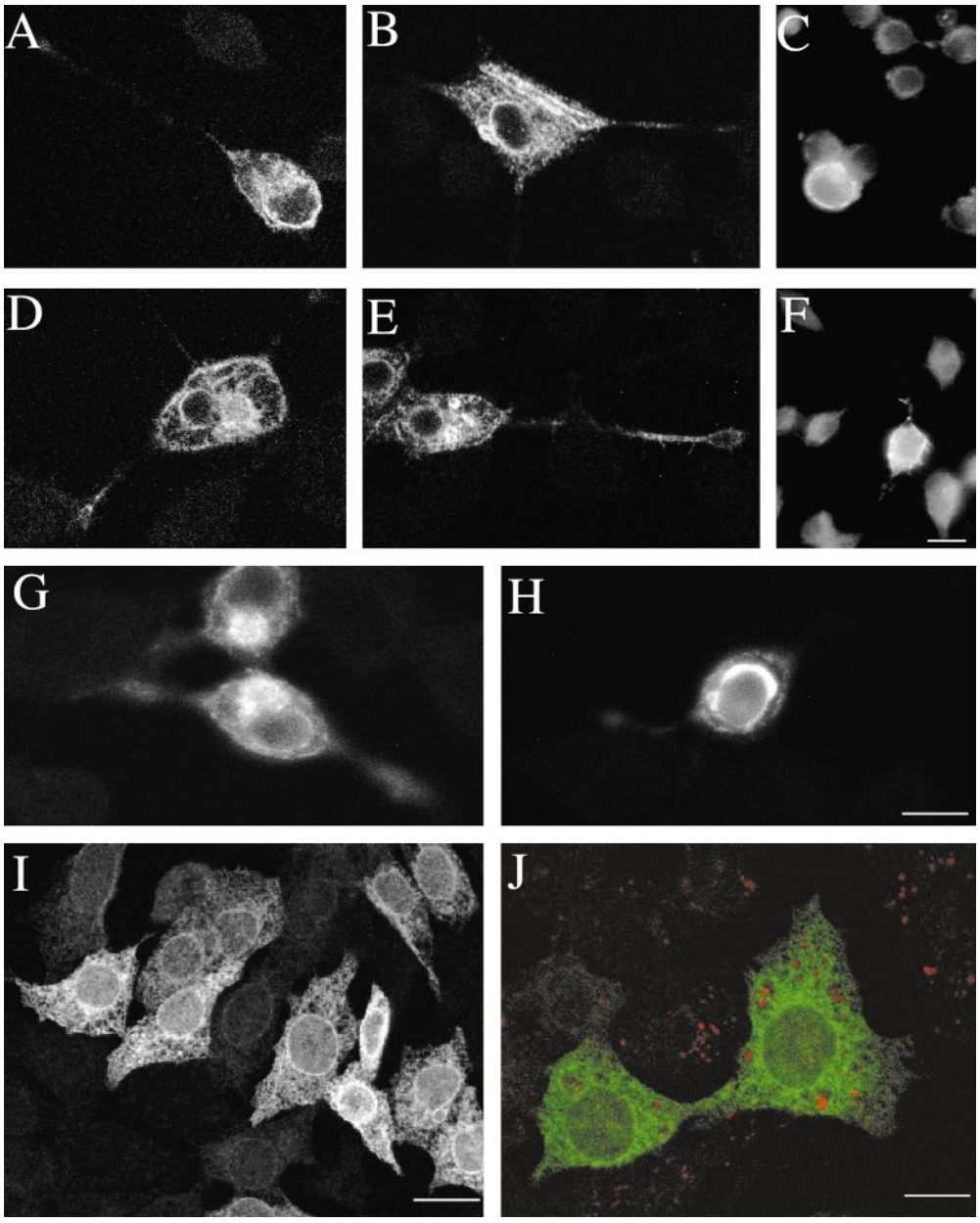

Figure 8. Confocal analysis of paranodin distribution in N2a cells when coexpressed with F3 mutated or chimeric constructs. N2a cells were transiently transfected with paranodin and a truncated form of F3 lacking the FNIII repeats (F3-Ig, A–C), a chimera between the Ig domains of TAG-1 and the FNIII domains of F3 (F3/TAG-1; D–F) or a secreted chimera between F3 and the Fc of human IgG devoid of GPI anchor (F3-Fc; G and H). 48 h after transfection, live cells were immunostained for F3 (C), or TAG-1 (F) to detect F3-Ig and F3/TAG-1 expression at the cell surface, respectively. Cells were fixed with methanol and immunostained for paranodin using an antiserum directed against the intracytoplasmic region (A, B, D, E, G, and H). None of the F3 deleted or chimeric constructs was able to reproduce the effect of F3 leading to paranodin expression at the plasma membrane (compare with Fig. 5, D and E). Experiments were performed in triplicate; 30–50 cells were analyzed in each experimental condition. I–J, Analysis of the intracellular distribution of paranodin in CHO cells expressing the truncated form of F3 lacking the FNIII repeats (clone B21). Paranodin was not expressed at the plasma membrane and appeared retained in the ER (I). Confocal analysis of double-immunofluorescence staining for paranodin (in green) and the Golgi complex marker giantin (in red; J) indicated that paranodin was not distributed in the Golgi complex. Bars: (A, B, D, E, G, H, I) 10 μm; (C and F) 20 μm; (J) 5 μm.

din was cotransfected with the F3-Ig construct, which contains the six Ig domains and the GPI anchor sequence, but not the FNIII repeats, a 95-kD band corresponding to F3-Ig was detected in the paranodin immune precipitate (Fig. 7 A). Thus, these data indicate that the Ig domains of F3 are sufficient for its cis-interaction with paranodin.

The FNIII Domains and GPI Anchor Are Required for the Association of F3 with Microdomains and Cell Surface Expression of Paranodin

We compared the role of the Ig and FNIII domains of F3 in mediating cell surface sorting of paranodin. N2a cells were cotransfected with paranodin and F3-Ig (Fig. 8, A and B) or F3/TAG-1 (Fig. 8, D and E) constructs (see Fig. 1). The F3/TAG-1 construct corresponds to the Ig domains of TAG-1 fused with the FNIII repeats and the GPI anchor of F3. Both F3-Ig and F3/TAG-1 molecules were expressed at the cell surface (Fig. 8, C and F). However, paranodin was found to remain intracellular in both conditions (>50 cells examined in each condition). Thus, the Ig region of F3 that associates with paranodin was unable to induce its cell surface expression in the absence of the FNIII domains of F3.

To understand why the association of paranodin with F3 deleted of the FNIII repeats was not sufficient to lead to the membrane delivery of paranodin, we tested whether F3-Ig was recovered in the TX-100–insoluble microdo-

mains. We used clones B21 and 1A, two stably-transfected clones of CHO cells that express similar amounts of GPI-anchored F3-Ig and F3, respectively, at the cell surface (Durbec et al., 1994). F3-Ig–expressing CHO cells were transiently transfected with paranodin and immunofluorescence staining showed that paranodin was not targeted to the cell surface (Fig. 8 I). Paranodin was distributed in the ER and did not colocalize with the Golgi complex (Fig. 8 J). F3-Ig–expressing CHO cells were extracted with TX-100 and subjected to a sucrose gradient centrifugation. As shown in Fig. 6 D, the F3-Ig molecule was exclusively found in the high density sucrose fractions. Therefore, the FNIII domains appeared to be crucial for the recruitment of the GPI-anchored F3 glycoprotein into microdomains and also for paranodin to be translocated from the ER to the Golgi compartment.

To assess the importance of the GPI anchor in generating the cell surface expression of paranodin, we used a secreted form of F3 that is fused with the Fc region of human IgG and lacks the GPI anchor (F3-Fc, see Fig. 1). As shown in Fig. 8, G and H, coexpression of F3Fc in double-transfected N2a neuroblastoma cells did not modify the intracellular distribution of paranodin. This result strongly suggests that the GPI anchor was also necessary for the correct transport of the F3/paranodin to the plasma membrane.

Discussion

Paranodin/caspr is a neuronal transmembrane glycoprotein that belongs to the neurexin superfamily and is enriched in the septate-like junctions of the paranodal regions of the nodes of Ranvier. It is related to *Drosophila* neurexin IV, which is highly enriched in septate junctions between epithelial cells where it appears to interact with coracle, a member of the band 4.1 family (Baumgartner et al., 1996). Interestingly, neurexin IV is also enriched in septate junctions between glial cells and, thus, paranodin and neurexin IV appear to play an evolutionary conserved role in axonal insulation. One characteristic of paranodin/caspr is its ability to associate with F3/contactin, a GPI-anchored axonal glycoprotein of the Ig superfamily, when the two proteins are expressed in the same cells (Peles et al., 1997). Although a previous report had concluded that contactin is not colocalized with caspr in paranodal junctions (Einheber et al., 1997), more recent work from the same group has contradicted these earlier findings and demonstrated that contactin is enriched in paranodal regions (Rios, J.C., M. Lustig, M. Grumet, L. Gollan, E. Peles, J.J. Hemperly, and J.L. Salzer. 1999. *Soc. Neurosci. Abstr.* 401.5). Thus, paranodin/caspr is likely to be associated with F3/contactin in most, if not all, instances. However, the functional significance of the interaction between F3 and paranodin had not been established.

The present study was aimed at understanding the role of F3 in the maturation of paranodin. Using cotransfection in CHO and neuroblastoma N2a cells, we found that when expressed alone, paranodin was not detected at the cell surface, but was retained in the ER. This retention is unlikely to be due to an interaction with the cytoskeleton through binding with band 4.1-like proteins, since it was also observed with a paranodin mutant deleted from its intracytoplasmic band 4.1-binding region (GNP motif). Therefore, the ectodomain of paranodin is likely to be responsible for its intracellular retention. The mechanism of this retention is not known. It could be secondary to an improper conformation of paranodin, to its interaction with trapping proteins, or its lack of interaction with transport proteins. Association with F3 glycoprotein led to surface expression of paranodin in double-transfected cells. This is, to our knowledge, the first demonstration for the surface sorting of a transmembrane molecule mediated by its cis-association with a GPI-linked glycoprotein. This finding raises the possibility that such a sorting mechanism could confer a new function to the lateral interaction that occurs between a variety of GPI-anchored and transmembrane molecules. F3 may modify the folding of paranodin and stabilize a transport-permissive conformation. It may also interfere with the complex that could be formed between paranodin and lectin-like chaperones of the ER, such as calnexin or calreticulin (Trombetta and Helenius, 1998). However, the specific requirement for paranodin sorting of domains of F3 that are not necessary for its interaction with paranodin suggests that the role of F3 is not only to play a role of chaperone or to prevent the interaction of paranodin with trapping proteins, but that it plays an active role in the trafficking of paranodin.

Several lines of evidence indicate that incorporation into lipid rafts is a necessary step for surface sorting of paranodin. First, paranodin was recruited to the TX-100–insoluble microdomains fraction when coexpressed with F3. Second, when the GPI anchor was deleted and F3 was expressed as a secreted Fc-chimera, paranodin was not transported to the cell surface. Third, a truncated form of F3 lacking the FNIII repeats, associated with paranodin, but was not partitioned to the lipid rafts and did not induce paranodin surface sorting. Thus, paranodin associated with F3 appears capable to be translocated from the ER to the Golgi compartment, before being incorporated into lipid rafts and transported to the cell surface. Indeed, removal of cholesterol with methyl β-cyclodextrin did not prevent the association between paranodin and F3, indicating that the two proteins can interact before their partitioning into the lipid rafts. The GPI anchor of F3 is necessary for this process since a soluble form of F3 was unable to achieve a proper targeting of paranodin to the membrane. In addition, our results demonstrate the importance of the FNIII repeats of F3 for both sorting F3 into microdomains and addressing the F3/paranodin complex to the membrane. Several mechanisms could account for the role of FNIII repeats. The FNIII domains may simply provide a spacer necessary for incorporation of F3 in lipid rafts. Alternatively, since this region is heavily glycosylated, the glycan content may be an important element for the targeting to microdomains. The existence of raft-associated lectins has been postulated that would be involved in clustering glycosylated proteins to mediate their apical delivery in epithelial cells (Simons and Ikonen, 1997). Such lectins could potentially also determine partitioning of glycoproteins into lipid rafts in nonpolarized cells.

Interestingly, the importance of FNIII repeats for addressing F3 to microdomains provides a possible explanation for their requirement for the association of F3 with signaling proteins. Previous studies demonstrated that an-

tibody-mediated cross-linking of F3, but not of the truncated F3-Ig form, expressed at the surface of CHO cells resulted in its association with Fyn kinase and the activation of protein tyrosine phosphorylation (Cervello et al., 1996). F3 was also shown to form a complex with Fyn into the TX-100–insoluble microdomains from postnatal mouse cerebellum (Olive et al., 1995). Microdomains have been proposed to provide membrane platforms, where interactions between GPI-anchored molecules, glycolipids, and signaling molecules take place after cellular activation or during transport (Sargiacomo et al., 1993; Simons and Ikonen, 1997). The results of the present study suggest that the lack of association with Fyn of the truncated F3-Ig form, could be secondary to its lack of sorting into microdomains. GPI-anchored molecules, such as F3, are likely to signal across the plasma membrane by lateral interaction with transmembrane coreceptor, as demonstrated in the case of the association of GDNF receptors with Ret (Jing et al., 1996). Paranodin/caspr has been proposed to be involved in transducing signal from F3/contactin, since its cytoplasmic COOH-terminal region contains a proline-rich sequence capable to bind in vitro GST-SH3 domains of Src and Fyn (Peles et al., 1997). Although the endogenous signaling proteins that bind paranodin remain to be identified, the F3-mediated recruitment of paranodin into microdomains could be a necessary condition for the association of the F3/paranodin complex with Src-family kinases. Recently, the protein tyrosine phosphatase, PTPα, has been reported as another possible transducing element associated in cis with F3/contactin (Zeng et al., 1999).

The immunoglobulin-like region of F3 appears sufficient for its interaction with paranodin, but not for the correct sorting of the complex formed by the two molecules. The F3-Ig domains are already known to interact with a large variety of structural motifs: the Ig domains of Nr-CAM and L1 (Brümmendorf et al., 1993; Morales et al., 1993), the FNIII repeats and the EGF domains of tenascin-R (Nörenberg et al., 1995; Xiao et al., 1996), and the carbonic anhydrase domain of RPTPβ/ζ and phosphacan (Peles et al., 1995). Moreover, when acting as a ligand expressed at the surface of CHO cells, the deleted F3-Ig form is capable to modulate neurite outgrowth like the whole F3 (Durbec et al., 1994; Buttiglione et al., 1996). In contrast, the FNIII repeats of F3 are not directly implicated in the binding of these extracellular ligands, and appear to provide a structural element that modifies the conformation of the protein and/or acts as a spacer (see above). The results of the present study strongly support such differential roles for the Ig and FNIII regions of F3, since the Ig region was sufficient for association with paranodin, whereas the FNIII domains were required for surface sorting of paranodin.

Although the functional relevance of the association between F3 and paranodin will have to be evaluated in vivo during the formation of Ranvier's nodes, our results suggest that the interaction between the two proteins is important for the correct maturation of paranodal junctions. The restricted expression of paranodin along nerve fibers at the paranodal junctions is progressively acquired during maturation both in vivo and in neuron–Schwann cell coculture (Menegoz et al., 1997; Einheber et al., 1997). Before myelination, paranodin is expressed diffusely in neurons, and uniformly distributed along neurites. Contacts between myelinating glial cells and axons induce the redistribution of paranodin that decreases in the internode region and becomes strikingly concentrated at the paranodes. Recently, F3/contactin was observed to be enriched in the paranodal region where it coclusters with paranodin/caspr with a similar time course during development of the rat sciatic nerve (Rios, J.C., M. Lustig, M. Grumet, L. Gollan, E. Peles, J.J. Hemperly, and J.L. Salzer. 1999. *Soc. Neurosci. Abstr.* 401.5). Therefore, it is likely that F3 is implicated in vivo in mediating the targeting of paranodin to the axonal membrane. In myelinated axons, sorting of paranodin may be achieved in two steps. First, paranodin associates with F3 and is addressed to the cell surface. Second, paranodin is clustered through interaction with Schwann cell/oligodendrocytes ligands and its lateral mobility becomes reduced. The role of glial cells in the clustering of paranodin to paranodes appears critical since the knockout of the cerebrogalactosyl-transferase gene, which is expressed in oligodendrocytes, results in the disruption of the paranodal regions and the uniform redistribution of paranodin along the axons (Dupree et al., 1999). However, beyond its implication in the maturation of paranodin, the role of F3 in mediating the clustering of paranodin in association with partners of the glial cell membrane remains to be established. F3/contactin may actually play multiple roles during the formation of the nodes of Ranvier, since it has been found to be transiently colocalized with sodium channels within the nodal gap in remyelinating axons (Kazarinova, K., Z.C. Xiao, E. Berglund, B. Ranscht, L. Gollan, E. Peles, L. Mattei, L. Isom, and P. Shrager. 1999. *Soc. Neurosci. Abstr.* 401.7). Moreover, the β2 subunit of the sodium channel contains an Ig domain with similarity to F3/contactin (Isom et al., 1995). Therefore, F3/contactin might play a role in the sodium channel expression at the cell surface or clustering at the nodal region. Finally, the phenotype of F3/contactin knockout mice has been recently reported. These mice display a severe ataxia and growth defects leading to death at postnatal day 18 (Berglund et al., 1999). This phenotype may only be partly accounted for by the reported defects in axonal and dendritic projections of cerebellar cells, and our results suggest that F3-deficient mice may have impaired sorting of paranodin, and, as a consequence, abnormal nodes of Ranvier.

We thank C. Moretti for confocal analysis and G. Gennarini and P. Durbec for helpful discussions.

This work was supported by the Association pour la Recherche sur la Sclérose En Plaques to C. Faivre-Sarrailh and EEC grant PL97-0329 to G. Rougon.

Submitted: 6 January 2000
Revised: 29 February 2000
Accepted: 3 March 2000

References

Baumgartner, S., J.T. Littleton, K. Broadie, M.A. Bhat, R. Harcke, J.A. Lengyel, R. Chiquet Ehrismann, A. Prokop, and H.J. Bellen. 1996. A *Drosophila* neurexin is required for septate junction and blood–nerve barrier formation and function. *Cell.* 13:1059–1068.

Bellen, H.J., Y. Lu, R. Beckstead, and M.A. Bhat. 1998. Neurexin IV, caspr and paranodin—novel members of the neurexin family: encounters of axons and glia. *Trends Neurosci.* 10:444–449.

Berglund, E.O., K. Murai, B. Fredette, G. Sekerkova, B. Marturano, L. Weber,

E. Mugnaini, and B. Ranscht. 1999. Ataxia and abnormal cerebellar microorganization in mice with ablated contactin gene expression. *Neuron*. 24: 739–750.

Brown, D., and J. Rose. 1992. Sorting of GPI-anchored proteins to glycolipid-enriched subdomains during transport to the apical surface. *Cell*. 68:533–544.

Brümmendorf, T., and F. Rathjen. 1996. Structure/function relationships of axon-associated adhesion receptors of the immunoglobulin superfamily. *Curr. Opin. Neurobiol*. 6:584–592.

Brümmendorf, T., M. Hubert, U. Treubert, R. Leuschner, A. Tarnok, and F. Rathjen. 1993. The axonal recognition molecule F11 is a multifunctional protein: specific domains mediate interactions with Ng-CAM and restrictin. *Neuron*. 10:711–727.

Buttiglione, M., J.M. Revest, G. Rougon, and C. Faivre-Sarrailh. 1996. F3 neuronal adhesion molecule controls outgrowth and fasciculation of cerebellar granule cell neurites: a cell-type specific effect mediated by the Ig-like domains. *Mol. Cell. Neurosci.* 8:53–69.

Buttiglione, M., J.M. Revest, O. Pavlou, D. Karagogeos, A. Furley, G. Rougon, and C. Faivre-Sarrailh. 1998. A functional interaction between the neuronal adhesion molecules TAG-1 and F3 modulates neurite outgrowth and fasciculation of cerebellar granule cells. *J. Neurosci.* 18:6853–6870.

Cervello, M., V. Matranga, P. Durbec, G. Rougon, and S. Gomez. 1996. The GPI-anchored adhesion molecule F3 induces tyrosine phosphorylation: involvement of the FNIII repeats. *J. Cell Sci.* 109:699–704.

Davis, J.Q., S. Lambert, and V. Bennett. 1996. Molecular composition of the node of Ranvier: identification of ankyrin-binding cell adhesion molecules neurofascin (mucin$^+$/third FNIII domain$^-$) and NrCAM at nodal axon segments. *J. Cell Biol.* 135:1355–1367.

Dupree, J.L., J.A. Girault, and B. Popko. 1999. Axo-glial interactions regulate the localization of axonal paranodal proteins. *J. Cell Biol.* 147:1145–1152.

Durbec, P., G. Gennarini, C. Goridis, and G. Rougon. 1992. A soluble form of the F3 neuronal cell adhesion molecule promotes neurite outgrowth. *J. Cell Biol*. 117:877–887.

Durbec, P., G. Gennarini, M. Buttiglione, S. Gomez, and G. Rougon. 1994. Different domains of the F3 neuronal adhesion molecule are involved in adhesion and neurite outgrowth promotion. *Eur. J. Neurosci.* 6:461–472.

Einheber, S., G. Zanazzi, W. Ching, S. Scherer, T. Milner, E. Peles, and J. Salzer. 1997. The axonal membrane protein Caspr, a homologue of neurexin IV, is a component of the septate-like paranodal junctions that assemble during myelination. *J. Cell Biol.* 139:1495–1506.

Faivre-Sarrailh, C., and G. Rougon. 1997. Axonal molecules of the immunoglobulin superfamily bearing a GPI anchor: their role in controlling neurite outgrowth. *Mol. Cell. Neurosci.* 9:109–115.

Furley, A.J., S.B. Morton, D. Manalo, D. Karagogeos, J. Dodd, and T.M. Jessell. 1990. The axonal glycoprotein TAG-1 is an immunoglobulin superfamily member with neurite outgrowth promoting activity. *Cell.* 61:157–170.

Gennarini, G., P. Durbec, A. Boned, G. Rougon, and C. Goridis. 1991. Transfected F3/F11 neuronal cell surface protein mediates intercellular adhesion and promotes neurites outgrowth. *Neuron*. 6:595–606.

Girault, J.A., G. Labesse, J.P. Mornon, and I. Callebaut. 1998. Janus kinases and focal adhesion kinases play in the 4.1 band: a superfamily of band 4.1 domains important for cell structure and signal transduction. *Mol. Med*. 4:751–769.

Girault, J.A., G. Labesse, J.P. Mornon, and I. Callebaut. 1999. The N-termini of FAK and JAKs contain divergent band 4.1 domains. *Trends Bioch. Sci.* 24: 54–57.

Isom, L.L., D.S. Ragsdale, K.S. De Jongh, R.E. Westenbroeck, B.F. Reber, T. Scheuer, and W.A. Catterall. 1995. Structure and function of the beta 2 subunit of brain sodium channels, a transmembrane glycoprotein with CAM motif. *Cell.* 83:433–442.

Jing, S., D. Wen, Y. Yu, P.L. Holst, Y. Luo, M. Fang, R. Tamir, L. Antonio, Z. Hu, R. Cupples, et al. 1996. GDNF-induced activation of the ret protein tyrosine kinase is mediated by GDNFR-alpha, a novel receptor for GDNF. *Cell.* 85:1113–1124.

Lambert, S., J.Q. Davis, and V. Bennett. 1997. Morphogenesis of the node of Ranvier: co-clusters of ankyrin and ankyrin-binding integral proteins define early developmental intermediates. *J. Neurosci.* 17:7025–7036.

Lisanti, M.P., M. Sargiacomo, L. Graeve, A. Saltiel, and E. Rodriguez-Boulan. 1989. Polarized apical distribution of glycosyl-phophatidylinositol-anchored proteins in a renal epithelial cell clone. *Proc. Natl. Acad. Sci. USA*. 85:9557–9561.

Menegoz, M., P. Gaspar, M. Le Bert, T. Galvez, F. Burgaya, C. Palfrey, P. Ezan, F. Arnos, and J.A. Girault. 1997. Paranodin, a glycoprotein of neuronal paranodal membranes. *Neuron*. 19:319–331.

Morales, G., M. Hubert, T. Brümmendorf, U. Treubert, A. Tarnok, U. Schwarz, and F. Rathjen. 1993. Induction of axonal growth by heterophilic interactions between the cell surface recognition proteins F11 and Nr-CAM/Bravo. *Neuron.* 11:1113–1122.

Nabi, I.R., A. Le Bivic, D. Fambrough, and E. Rodriguez-Boulan. 1991. An endogenous MDCK lysosomal membrane glycoprotein is targeted basolaterally before delivery to lysosomes. *J. Cell Biol*. 115:1573–1584.

Nörenberg, U., M. Hubert, T. Brümmendorf, A. Tarnok, and F.G. Rathjen. 1995. Characterization of functional domains of the tenascin-R (restrictin) polypeptide–cell attachment site, binding with F11, and enhancement of F11-mediated neurite outgrowth by tenascin-R. *J. Cell Biol.* 130:473–484.

Olive, S., C. Dubois, M. Schachner, and G. Rougon. 1995. The F3 neuronal GPI-linked molecule is localized to glycolipid-enriched membrane subdomains and interacts with L1 and fyn-kinase in cerebellum. *J. Neurochem*. 65: 2307–2317.

Peles, E., M. Nativ, P.L. Campbell, R. Sakurai, R. Martinez, S. Lev, D.O. Clary, J. Schilling, G. Barnea, G.D. Plowman, M. Grumet, and J. Schlessinger. 1995. The carbonic anhydrase domain of receptor tyrosine phosphatase beta is a functional ligand for the axonal cell recognition molecule contactin. *Cell.* 82:252–260.

Peles, E., M. Nativ, M. Lustig, M. Grumet, J. Schilling, R. Martinez, G.D. Plowman, and J. Schlessinger. 1997. Identification of a novel contactin-associated transmembrane receptor with multiple domains implicated in protein–protein interactions. *EMBO (Eur. Mol. Biol. Organ.) J.* 16:978–988.

Poliak, S., L. Gollan, R. Martinez, A. Custer, S. Einheber, J.L. Salzer, J.S. Trimmer, P. Shrager, and E. Peles. 1999. Caspr2, a new member of the neurexin superfamily, is localized at the juxtaparanodes of myelinated axons and associates with K^+ channels. *Neuron*. 24:1037–1047.

Revest, J.M., C. Faivre-Sarrailh, N. Maeda, M. Noda, M. Schachner, and G. Rougon. 1999. The interaction between F3 immunoglobulin domains and protein tyrosine phosphatases z/β triggers bidirectional signalling between neurons and glial cells. *Eur. J. Neurosci.* 11:1134–1147.

Sargiacomo, M., M. Sudol, T.I. Tang, and M. Lisanti. 1993. Signal transducing molecules and glycosyl-phosphatidylinositol-linked proteins form a caveolin-rich insoluble complex in MDCK cells. *J. Cell Biol.* 122:789–807.

Simons, K., and E. Ikonen. 1997. Functional rafts in cell membranes. *Nature.* 387:569–572.

Trombetta, E.S., and A. Helenius. 1998. Lectins as chaperones in glycoprotein folding. *Curr. Opin. Struct. Biol.* 8:587–592.

Volkmer, H., R. Leuschner, U. Zacharias, and F. Rathjen. 1996. Neurofascin induces neurites by heterophilic interactions with axonal NrCAM while NrCAM requires F11 on the axonal surface to extend neurites. *J. Cell Biol*. 135:1059–1069.

Volkmer, H., U. Zacharias, U. Nörenberg, and F. Rathjen. 1998. Dissection of complex molecular interactions of neurofascin with axonin-1, F11, and tenascin-R, which promote attachment and neurite formation of tectal cells. *J. Cell Biol.* 142:1083–1093.

Wang, H., D.D. Hunkel, T.M. Martin, P.A. Schwartzkroin, and B.L. Tempel. 1993. Heteromultimeric K+ channels in terminal and juxta-paranodal regions of neurons. *Nature.* 365:75–79.

Waxman, S.G., and J.M. Ritchie. 1993. Molecular dissection of the myelinated axon. *Ann. Neurol.* 33:121–136.

Xiao, Z.C., J. Taylor, D. Montag, G. Rougon, and M. Schachner. 1996. Distinct effects of recombinant tenascin-R domains in neuronal cell functions and identification of the domain interacting with the neuronal recognition molecule F3/11. *Eur. J. Neurosci.* 8:766–782.

Xiao, Z.C., D.S. Ragsdale, J.D. Malhotra, L.N. Mattei, P.E. Braun, M. Schachner, and L.L. Isom. 1999. Tenascin-R is a functional modulator of sodium channel beta subunits. *J. Biol. Chem*. 274:26511–26517.

Yuan, L.L., and B. Ganetzky. 1999. A glial–neuronal signaling pathway revealed by mutations in a neurexin-related protein. *Science.* 283:1343–1345.

Zeng, L., L. D'alessandri, M.B. Kalousek, L. Vaughan, and C.J. Pallen. 1999. Protein tyrosine phosphatase α (PTPα) and contactin form a novel neuronal receptor complex linked to the intracellular tyrosine kinase fyn. *J. Cell Biol*. 147:707–713.

Zhang, X., and V. Bennett. 1998. Restriction of 480/270-kD ankyrin G to axon proximal segments requires multiple ankyrin G-specific domains. *J. Cell Biol*. 142:1571–1581.